

Design of non-isomorphic symmetric descendants of the Miura-ori

This content has been downloaded from IOPscience. Please scroll down to see the full text.

2015 Smart Mater. Struct. 24 085002

(<http://iopscience.iop.org/0964-1726/24/8/085002>)

View [the table of contents for this issue](#), or go to the [journal homepage](#) for more

Download details:

IP Address: 129.169.70.132

This content was downloaded on 15/06/2016 at 12:23

Please note that [terms and conditions apply](#).

Design of non-isomorphic symmetric descendants of the Miura-ori

Pooya Sareh and Simon D Guest

University of Cambridge, UK

E-mail: p.sareh@imperial.ac.uk

Received 8 March 2015, revised 17 May 2015

Accepted for publication 19 May 2015

Published 30 June 2015



CrossMark

Abstract

The Miura fold pattern, or the Miura-ori, is a flat-foldable origami pattern with various applications in engineering and architecture. In addition to free-form variations, scholars have proposed a number of symmetric derivatives for this classic fold pattern over recent years. In a previous work, the authors of this paper studied isomorphic variations on the Miura-ori which led to the development of an ‘isomorphic family’ for this fold pattern. In this paper, we study non-isomorphic variations on the Miura-ori in order to develop a ‘non-isomorphic family’ for this pattern. Again we start with the Miura-ori, but reduce the symmetry by migrating from the original symmetry group to its subgroups, which may also include the enlargement of its unit cell. We systematically design and classify the non-isomorphic symmetric descendants of the Miura-ori which are either globally planar, or globally curved, flat-foldable tessellations.

Keywords: origami, the Miura-ori, flat-foldability, symmetry, wallpaper groups

(Some figures may appear in colour only in the online journal)

1. Introduction

The Miura-ori is a globally planar [1] flat-foldable origami tessellation with a wide range of engineering applications (see, e.g., [2]). It has been shown [3] that the symmetry group of the Miura fold pattern is pmg , which is one of the seventeen wallpaper (or plane symmetry) groups. Two wallpaper patterns are said to be *isomorphic* if they belong to the same symmetry group, although they may have different unit cells. Otherwise, the patterns are said to be *non-isomorphic*. The authors of this paper have developed a framework [1] for the symmetric generalization of the Miura-ori and studied isomorphic variations [4] on this pattern which resulted in the design and development of an ‘isomorphic family’ for this fold pattern. In developing this family, to obtain less symmetric flat-foldable patterns, we used systematic enlargements on the unit cell of the Miura-ori, while at the same time preserving the plane symmetry group.

It has been shown (see, e.g., [5]) that there are exactly seventeen distinct wallpaper groups. Figure 1 shows the international notation for the seven wallpaper groups which we deal with in this paper (see [6] or [7] for all the seventeen groups). Note that only rotation centres of order 2, 3, 4, or 6 (i.e. rotations by 180°, 120°, 90°, or 60°, respectively) can

exist in a planar tessellation, which is known as the ‘crystallographic restriction’ [8, 9]. There are subgroup relationships [10] among the seventeen wallpaper groups. For example, the group pm is a subgroup of the group pmg , since we can remove some symmetry elements from the pmg unit cell and obtain a pm unit cell. The group pmg is called a supergroup for the group pm . This discussion implies that every pmg wallpaper pattern can be considered to be a pm pattern; however, pm is not the *maximal* symmetry group for a pmg pattern. In this study, we generally describe the maximal symmetry group of a pattern to be its symmetry group. Sometime, more explicitly, we describe the symmetry as being *strictly* the maximal symmetry.

In this paper, we explore non-isomorphic variations on the Miura-ori in order to develop a ‘non-isomorphic family’ for this fold pattern. Again we start with the Miura-ori, but reduce the symmetry by migrating from pmg to its subgroups, which may also include the enlargement of its unit cell. By ‘enlargement’ we imply putting together a number of adjacent unit cells to form a larger unit cell which provides us with more degrees of freedom which we use to develop design variations on the original pattern. According to the subgroup relationships among the seventeen

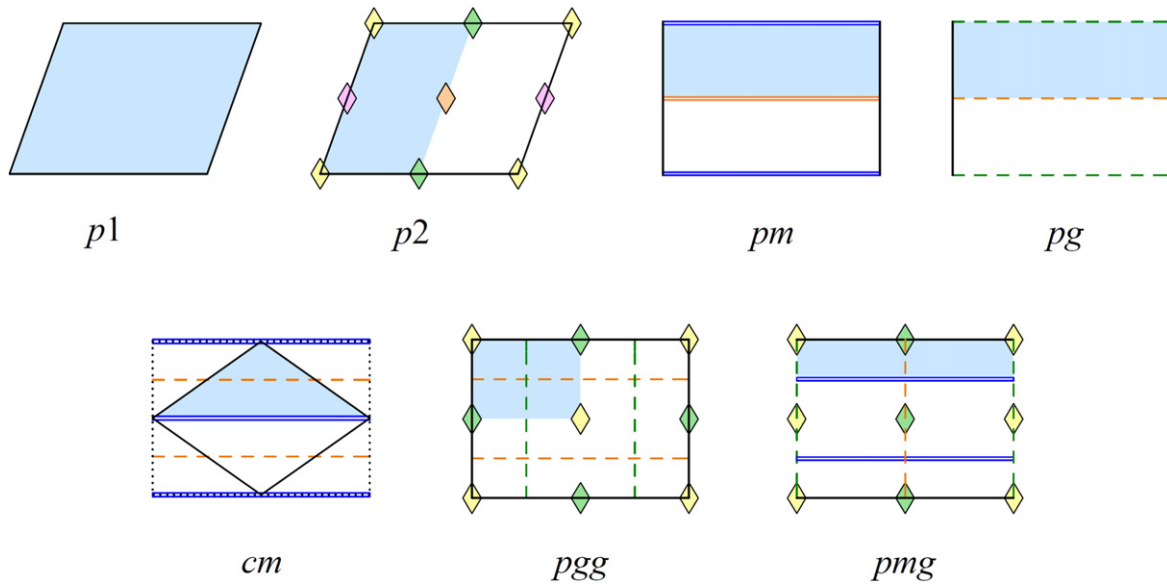


Figure 1. International notation for the seventeen plane symmetry groups (adapted from [7]). Bold black lines represent the outline of unit cells. Double and dashed lines represent reflection and glide reflection axes, respectively. 2-fold axes are shown by rhombuses. The blue shaded area shows the fundamental region of the pattern. Different colours for a symmetry element represent different classes of that element in the pattern. Dotted lines for the *cm* unit cell represent the outline of its *centred cell* [7] which contains two unit cells.

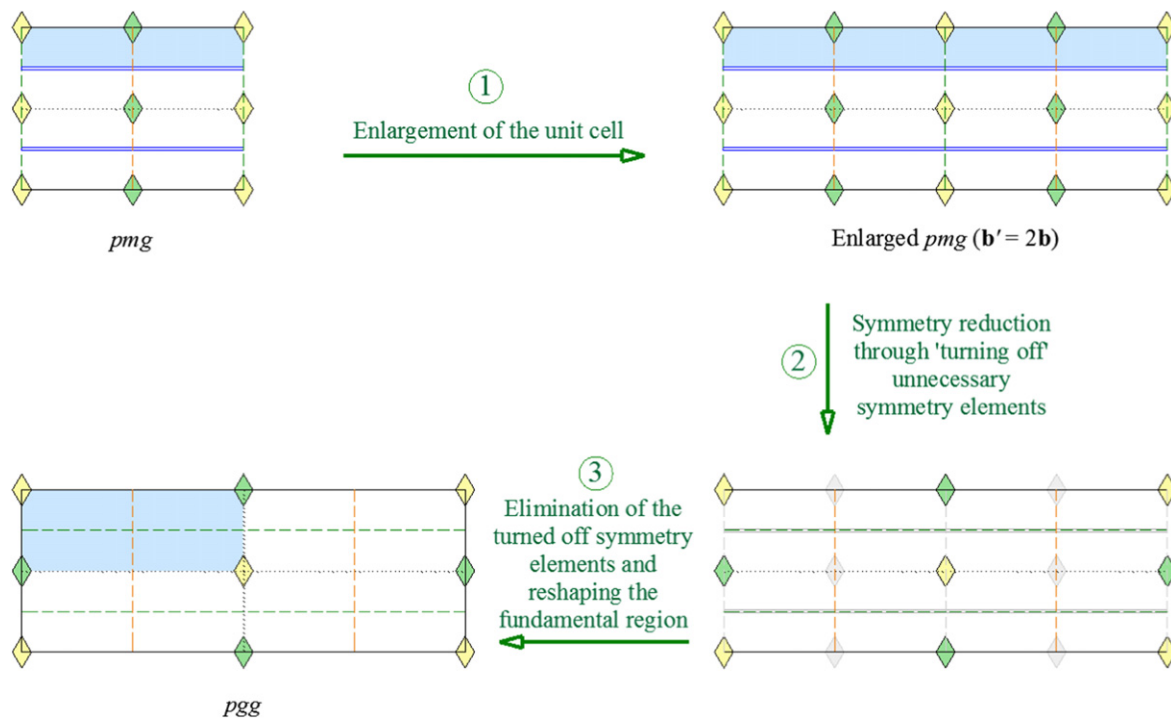


Figure 2. The transformation process of a *pmg* unit cell into a *pgg* unit cell, which includes a unit cell enlargement. The symmetry elements which are turned off are shown in grey.

wallpaper groups [10, 11], the non-isomorphic subgroups of *pmg* are *pgg*, *pg*, *cm*, *pm*, *p2* and *p1*. Three of these six groups have rectangular unit cells, which are *pgg*, *pg* and *pm*. We start with the most symmetric subgroup, i.e. *pgg*, and carry on the study for the subgroups *pg* and *pm*. Then we study the other three subgroups of *pmg*, i.e. *cm*, *p2*, and *p1*, which have non-rectangular unit cells. The naming scheme is based on Definition 1 in [4].

2. Non-isomorphic descendants with rectangular unit cells

2.1. Group *pgg*

Consider a *pmg* unit cell with lattice translation vectors **a** and **b**. According to the International Tables for Crystallography [6], the maximal *pgg* subgroup for this group has a unit cell

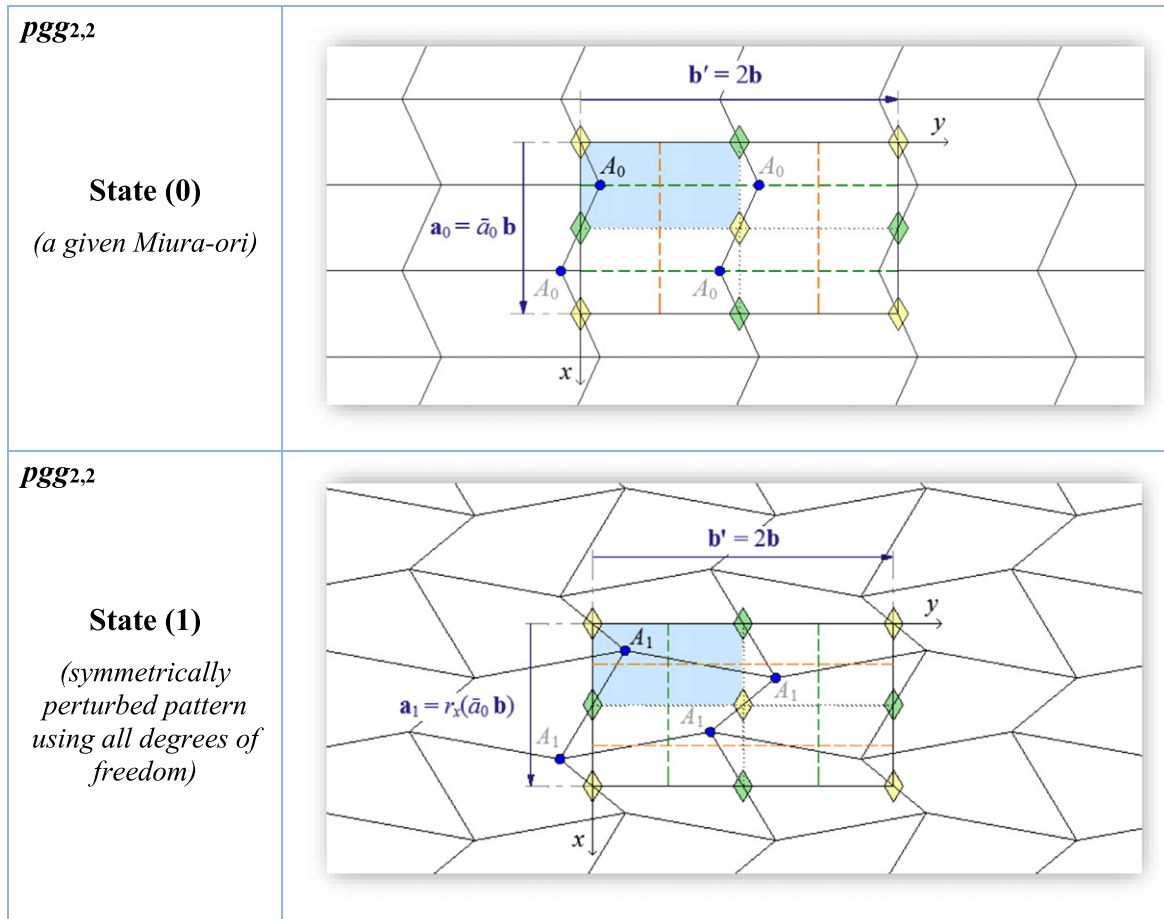


Figure 3. A $pgg_{2,2}$ variation of the Miura-ori. State (0): a given Miura fold pattern. State (1): a symmetrically perturbed state using all degrees of freedom. State (1) is not flat-foldable in general; we present a flat-foldable variation of it later in this section.

with $\mathbf{b}' = 2\mathbf{b}$. It implies that a $pgg_{m,1}$ variation of the Miura-ori (for any natural number m) does not exist, as a pmg unit cell with only one quadrilateral in the y -direction cannot be considered to be a strictly pgg unit cell.

Figure 2 shows the transformation process of a pmg unit cell into a pgg unit cell. A pmg group can be transformed into a pgg group through a *symmetry reduction transformation*. In figure 2, this transformation is illustrated in three steps. In the first step, we enlarge the unit cell to obtain a unit cell with $\mathbf{b}' = 2\mathbf{b}$. In the second step, we ‘turn off’ all unnecessary symmetry elements. The symmetry elements which are turned off are shown in grey. In this case, we have turned off the reflection axis, as well as unnecessary 2-fold and glide reflection axes. It should be noted that a glide reflection axis is added over the reflection axis which is turned off, as a reflection axis can also be considered to be a glide reflection axis. It should be also noted that the retained 2-fold axes have been re-grouped according to the pgg standard unit cell through changing their face colour. In the third step, we eliminate all the symmetry elements which are turned off, and reshape the fundamental region of the transformed unit cell.

2.1.1. Design variation analysis of $pgg_{2,2}$. As mentioned earlier, the maximal pgg subgroup of pmg has a unit cell with $\mathbf{b}' = 2\mathbf{b}$. For a Miura fold pattern, this unit cell, which is called

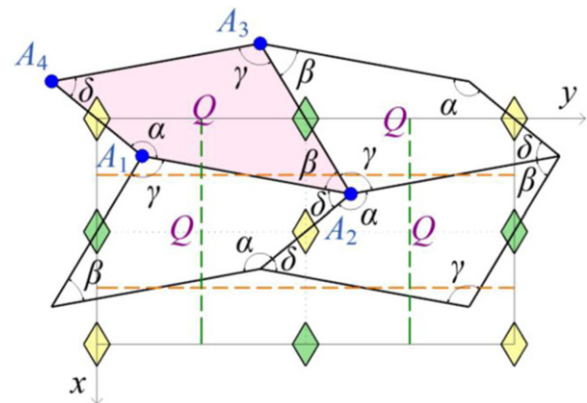


Figure 4. A set up of four adjacent quadrilaterals from State (1) of the previous figure.

$pgg_{2,2}$, is depicted in figure 3, State (0). There is only one orbit of nodes associated with the unit cell, shown as A_0 (the position of every node in an orbit is defined by symmetry operations from the position of any one node within the orbit). Since we are dealing with a pgg group, we have a degree of freedom for the aspect ratio of the unit cell. We are allowed to move node A_0 in the x - or y -directions. Note here that the glide reflection axis does not constrain the node in the way

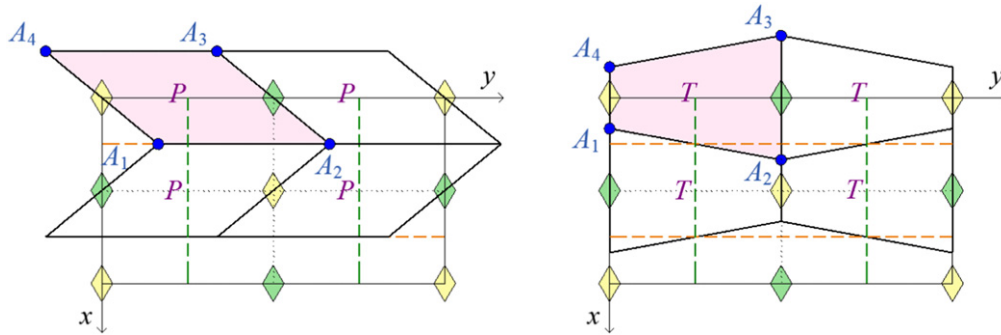


Figure 5. The two possible solutions from applying the flat-foldability condition at vertex A_2 to the previous figure. Labels P and T denote parallelogram and trapezoid, respectively.

that a reflection axis would. As node A_0 is a generic node, there is a constraint equation due to the flat-foldability condition at this node. In the lower part of figure 3, we have perturbed the pattern using all the degrees of freedom that we introduced earlier to obtain a new configuration, State (1).

In order to investigate the application of the flat-foldability condition to the pattern at node A_1 , we have illustrated a set up of four adjacent congruent quadrilaterals associated with a unit cell, from State (1) of the previous figure, in figure 4. For clarity, as we are now dealing with a geometric problem, we ignore the naming scheme for symmetrically equivalent nodes associated with a unit cell. We have renamed the vertices of the shaded quadrilateral as A_1, A_2, A_3 and A_4 . Note that, symmetrically, all these nodes are equivalent.

According to figure 4, side A_3A_4 is a glide-reflection of side A_1A_2 , with regard to the green glide reflection axis on the left. Therefore:

$$A_1A_2 = A_3A_4. \tag{1}$$

Applying the flat-foldability constraint at vertex A_2 , we conclude that:

$$\alpha + \beta = \pi. \tag{2}$$

This implies that:

$$A_1A_4 \parallel A_2A_3 \tag{3}$$

which means that Q is a trapezoid. In addition, from equation (1) we can conclude that Q must be an isosceles trapezoid, which includes parallelograms. (In dealing with quadrilaterals, we consider the inclusive definition for a trapezoid, in which a quadrilateral with at least one pair of parallel sides is a trapezoid. According to this definition, a parallelogram is a special case of trapezoid. Trapezoids with exactly one pair of parallel sides are called *strict trapezoids*. In this paper, unless otherwise stated, we consider the inclusive definition for a trapezoid).

According to the above discussion, the starting quadrilateral of a $pgg_{2,2}$ variation of the Miura-ori must be either a parallelogram, or an isosceles trapezoid. (Note that parallelograms include rectangles, rhombuses and squares, among which, only rhombuses can generate legitimate variations [1] of the Miura-ori). These solutions are depicted in figure 5. In the first case, the pattern is a Miura-ori, and in the second

case, it is not a legitimate variation of the Miura pattern. This discussion concludes that a flat-foldable $pgg_{2,2}$ variation of the Miura-ori does not exist.

2.1.2. Design variation analysis of $pgg_{2,2}^+$. We showed in the previous section that a flat-foldable $pgg_{2,2}$ variation of the Miura-ori does not exist. However, starting from the alternative standard unit cell, S^+ (see [1] or [4]), we can design a $pgg_{2,2}^+$ variation of the Miura-ori, which turns out to be always flat-foldable. Figure 6 illustrates this design variation. We have illustrated a set up of four adjacent parallelograms associated with a unit cell, from State (1) of the previous figure, in figure 7. As revealed by this figure, the flat-foldability condition at node A is always satisfied. Therefore, all the $pgg_{2,2}^+$ variations of the Miura-ori are flat-foldable. Also, they are all globally planar. An example for $pgg_{2,2}^+$ is shown in figure 8. It consists of two different starting parallelograms, shown as P_1 and P_2 .

In order to continue exploring the minimal pgg variations of the Miura-ori, the next section discusses the pgg variation with minimal enlargement of the unit cell in both x - and y -directions.

2.1.3. Design variation analysis of $pgg_{6,2}$. Consider a pmg unit cell with lattice translation vectors \mathbf{a} and \mathbf{b} . As discussed in the previous section, the maximal pgg subgroup for this group has a unit cell with $\mathbf{b}' = 2\mathbf{b}$. Having shown that a $pgg_{2,2}$ variation of the Miura-ori does not exist, we intend to design a variation of the Miura-ori by applying a minimal enlargement on the $pgg_{2,2}$ unit cell. According to the International Tables for Crystallography [6], the minimal enlargement in the x -direction which retains the symmetry group of a pgg pattern is $\mathbf{a}' = 3\mathbf{a}$. For a Miura fold pattern, this unit cell is called $pgg_{6,2}$. A $pgg_{6,2}$ unit cell is illustrated in figure 9. There are three distinct orbits of generic nodes associated with the unit cell, shown as A, B and C .

In order to investigate the application of the flat-foldability condition to the pattern, we have illustrated the fundamental region of a typical $pgg_{6,2}$ variation of the Miura-ori accompanied by its surrounding fold lines in figure 10. The grey nodes in the previous figure have been distinguished from each other by asterisk (*), dagger (†), and double dagger (‡), in this figure.

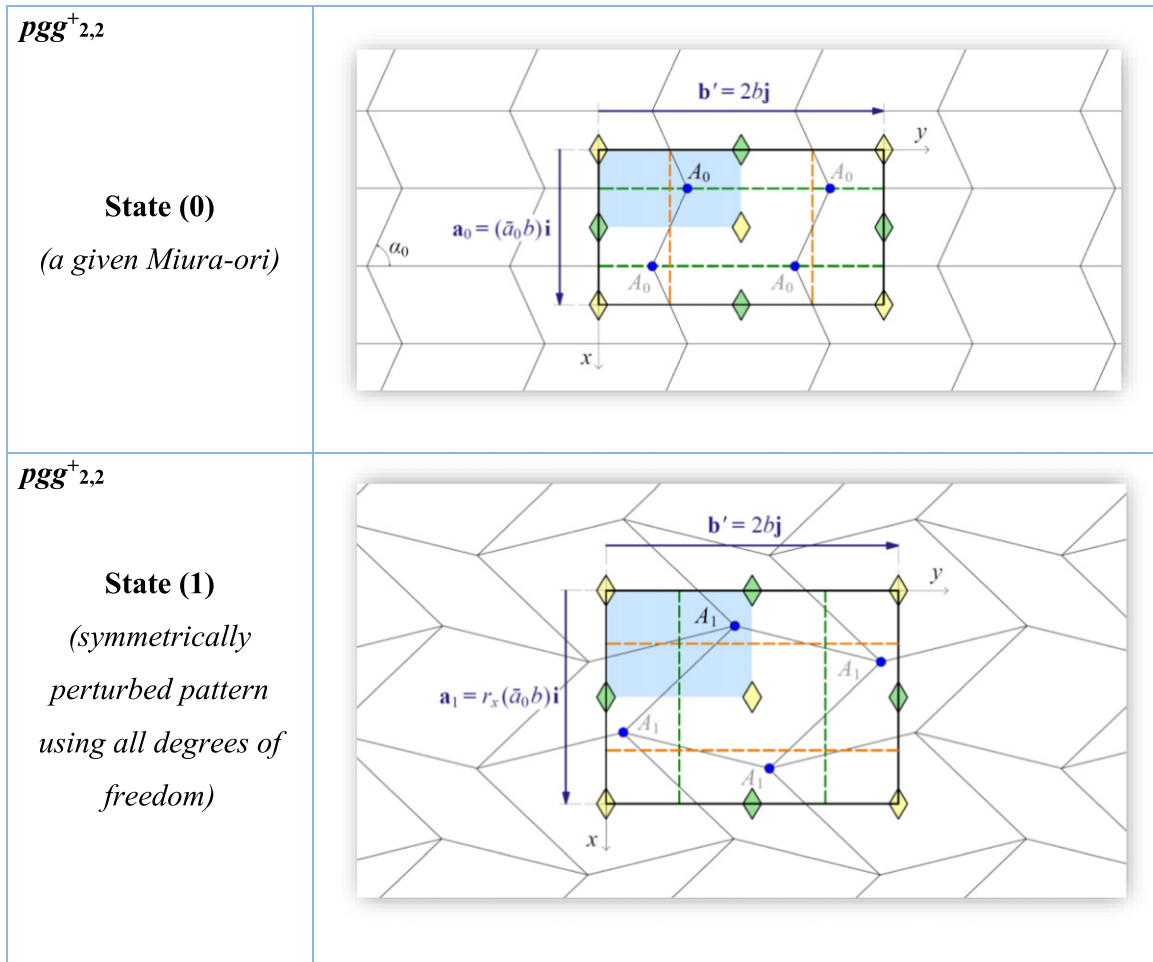


Figure 6. A $pgg_{2,2}^+$ variation of the Miura-ori. State (0): a given Miura fold pattern. State (1): a symmetrically perturbed state using all degrees of freedom.

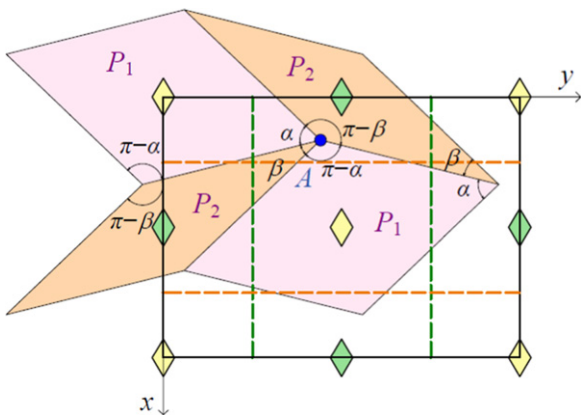


Figure 7. A set up of four adjacent parallelograms from State (1) of the previous figure.

Applying the flat-foldability condition at node C^* yields:

$$\angle C_2^* + \angle C_4^* = \pi. \tag{4}$$

We know that, because of the symmetry, $\angle C_4 = \angle C_4^*$. Hence:

$$\angle C_2^* + \angle C_4 = \pi. \tag{5}$$

This implies that:

$$AC \parallel BC^* \tag{6}$$

which means that Q_2 is a trapezoid. This also implies that (note that glide-reflection is an angle-preserving transformation):

$$CB^* \parallel C^*A^* \tag{7}$$

which means that Q_3 is a trapezoid.

Now we explore the geometry of quadrilateral Q_1 . From $AC \parallel BC^*$ we can conclude:

$$\angle A_4 + \angle B_3 = \pi. \tag{8}$$

On the other hand, applying the flat-foldability constraint at nodes A and B , respectively, we obtain:

$$\angle A_2 + \angle A_4 = \pi, \tag{9}$$

$$\angle B_1 + \angle B_3 = \pi. \tag{10}$$

Substituting $\angle A_4$ and $\angle B_3$ from equations (9) and (10), respectively, into equation (8), gives:

$$\angle A_2 + \angle B_1 = \pi. \tag{11}$$

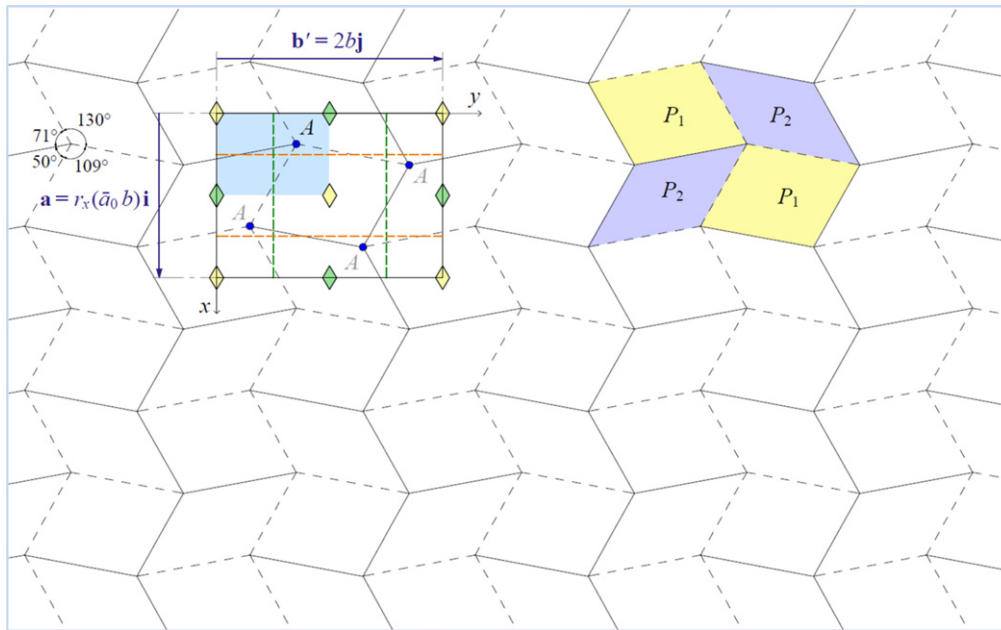


Figure 8. An example for a $pgg_{2,2}^+$ variation of the Miura-ori. It consists of two different starting parallelograms, shown as P_1 and P_2 . Solid lines show mountain fold lines, while dashed lines represent valley fold lines.

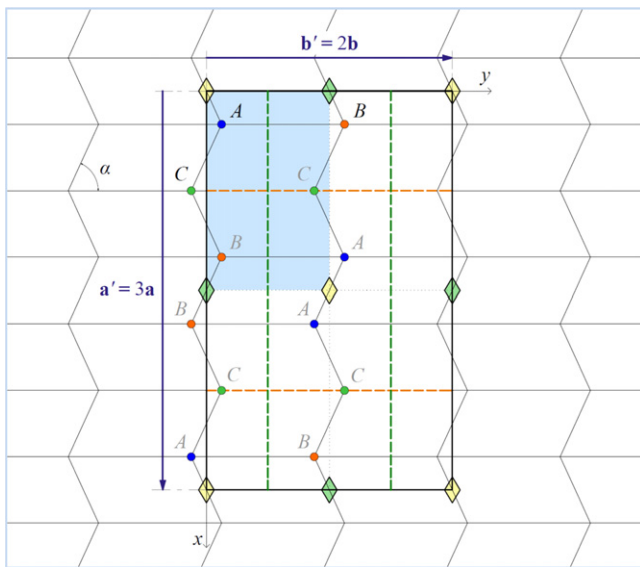


Figure 9. From a symmetry point of view, a $pgg_{6,2}$ unit cell contains three distinct orbits of nodes, shown as A , B and C .

Replacing $\angle A_2$ and $\angle B_1$ by their respective symmetry equivalents gives us:

$$\angle A_2^\ddagger + \angle B_1^\ddagger = \pi. \tag{12}$$

This implies that:

$$A^\ddagger A || B^\ddagger B \tag{13}$$

which means that Q_1 is a trapezoid. This also implies that:

$$\angle A_1 + \angle B_2 = \pi. \tag{14}$$

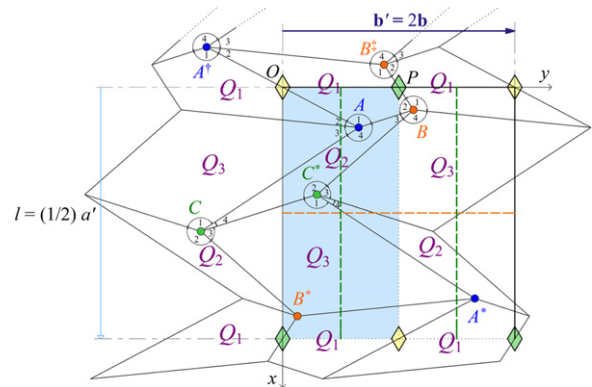


Figure 10. The fundamental region of a typical $pgg_{6,2}$ variation of the Miura-ori along with its surrounding crease lines. The grey nodes in the previous figure have been marked by asterisk, dagger, and double dagger, in this figure.

Combining equations (9) and (10) with equation (11) gives:

$$\angle A_2 = \angle B_3, \tag{15}$$

$$\angle A_4 = \angle B_1. \tag{16}$$

We also know from the flat-foldability condition at nodes A and B , respectively:

$$\angle A_1 + \angle A_3 = \pi, \tag{17}$$

$$\angle B_2 + \angle B_4 = \pi. \tag{18}$$

Combining equations (17) and (18) with equation (14) gives:

$$\angle A_3 = \angle B_2, \tag{19}$$

$$\angle A_1 = \angle B_4. \tag{20}$$

From equations (15), (16), (19) and (20) we obtain an interesting result: the two nodes A and B are geometrically

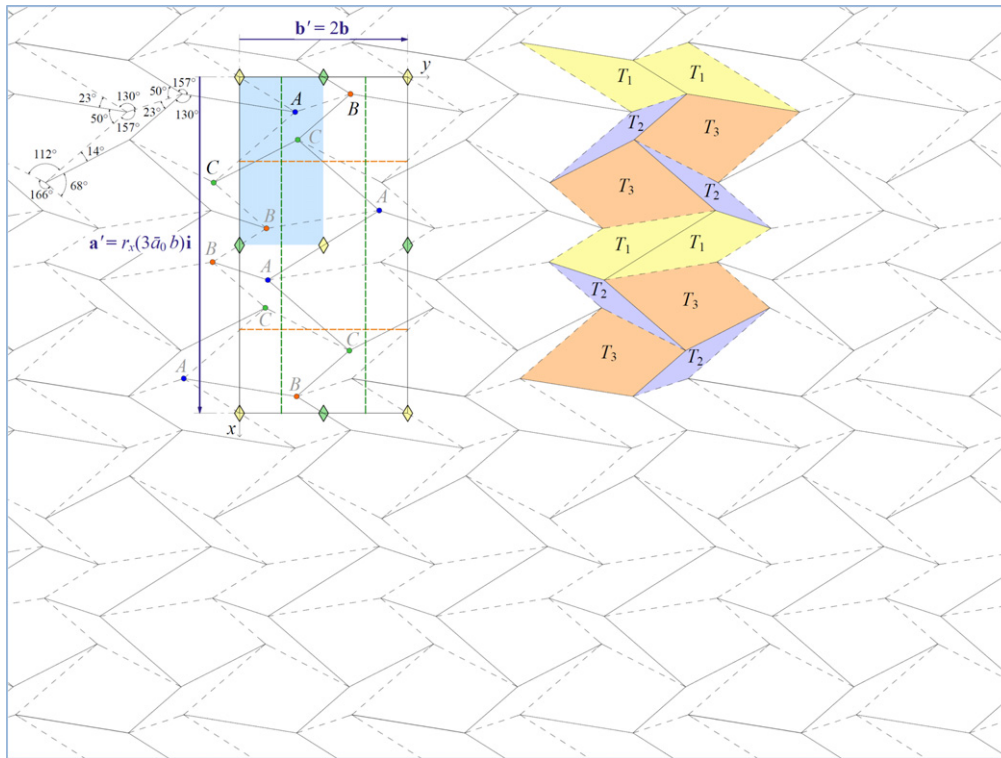


Figure 11. An example for a flat-foldable $pgg_{6,2}$ variation of the Miura-ori. It consists of three different starting trapezoids, shown as T_1 , T_2 and T_3 . Solid lines show mountain fold lines, while dashed lines represent valley fold lines.

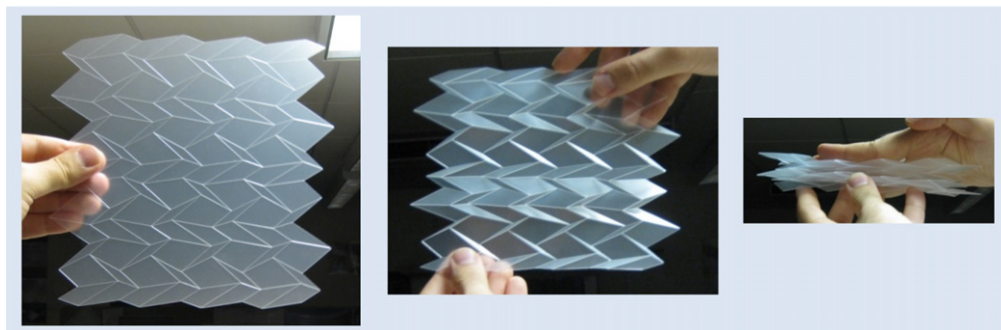


Figure 12. A polypropylene model of the fold pattern depicted in the previous figure [12].

congruent. Despite their congruency, they are distinct points from a symmetry point of view, as they do not belong to the same orbit. In other words, they are not related to each other by the symmetry elements of the pattern. In summary, geometrically, there are two types of nodes in a planar $pgg_{6,2}$ variation of the Miura fold pattern: a generic node A or B , and a generic node C .

Figure 11 shows an example for a flat-foldable $pgg_{6,2}$ variation of the Miura fold pattern alongside the assigned mountains and valleys. The pattern consists of three different starting trapezoids, shown as T_1 , T_2 and T_3 . In order to have a globally planar variation of the Miura-ori, we need to have all transverse polylines piecewise parallel. As can be deduced from equations (6), (7), and (13), this condition is satisfied in

all $pgg_{6,2}$ variations of the Miura-ori. As a result, all the $pgg_{6,2}$ variations of the Miura-ori are globally planar.

The $pgg_{6,2}$ variation of the Miura-ori is a globally planar pattern which folds to a frieze pattern, without having any (globally) straight longitudinal polyline. In other words, we have managed to replace the straight longitudinal lines in the Miura fold pattern by a pair of alternating polylines, while preserving the global planarity of the pattern. Figure 12 shows a polypropylene model of the fold pattern depicted in figure 11.

Starting from the alternative standard unit cell, we can design a 6×2 isomorphic variation of the Miura-ori, $pgg_{6,2}^+$, which is different from $pgg_{6,2}$. We have shown [13] that all the $pgg_{6,2}^+$ variations of the Miura-ori are globally planar.

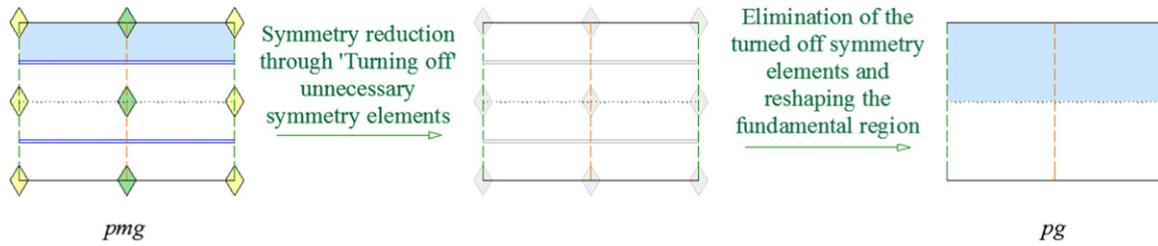


Figure 13. The transformation process of a pmg unit cell into a pg unit cell. The symmetry elements which are turned off are shown in grey.

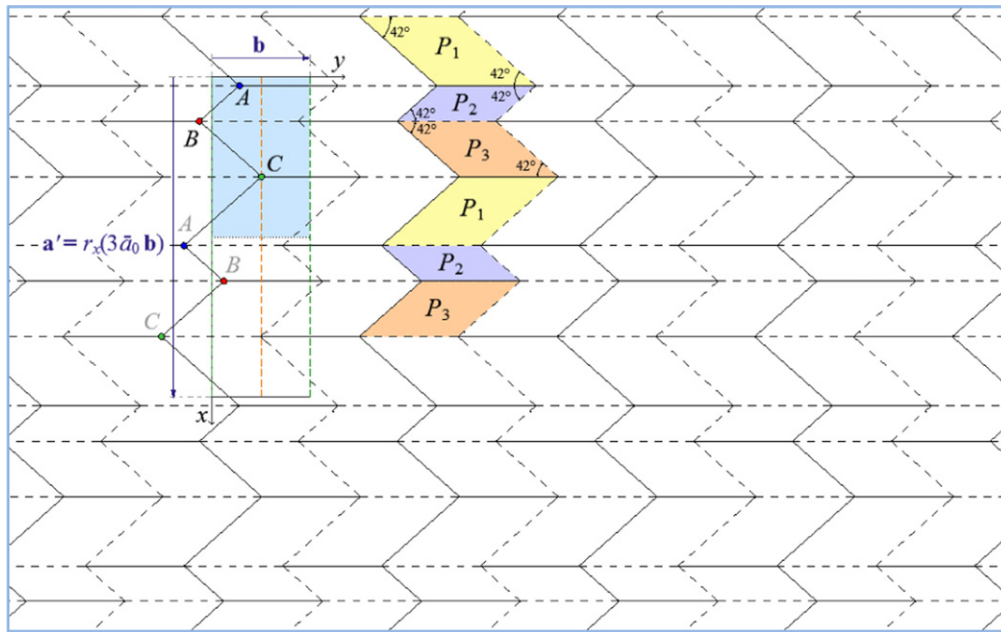


Figure 14. An example for a flat-foldable $pg_{6,1}$ variation of the Miura-ori. It consists of three different starting parallelograms, shown as P_1 , P_2 and P_3 . Solid lines show mountain fold lines, while dashed lines represent valley fold lines.

2.2. Group pg

Figure 13 shows the unit cell of a pmg wallpaper group versus the unit cell of a pg wallpaper group. The symmetry reduction transformation is illustrated in two steps. In the first step, we turn off all unnecessary symmetry elements. In this case, we have turned off the 2-fold axes, as well as the reflection axis, while retaining the glide reflection axes. In the second step, we eliminate all the symmetry elements which are turned off, and reshape the fundamental region of the transformed unit cell.

In order to have vertical glide reflection axes in the study of pg descendants of the Miura-ori, we use a 90° rotated version of the ITC standard pg unit cell. The reason is that since we intend to retain the pmg unit cell of the Miura-ori, in which the glide reflection axes are vertical, as a reference for our variations, tracking the changes through the symmetry reduction process is easier when glide reflection axes are vertical.

An extensive study of the minimal pg variations of the Miura-ori is presented in [13], proving that flat-foldable $pg_{2,1}$, $pg_{2,2}$ and $pg_{2,2}^+$ variations of the Miura-ori do not exist. Figure 14 shows a flat-foldable $pg_{6,1}$ variation of the Miura fold pattern alongside the assigned mountains and valleys.

The pattern consists of three different starting parallelograms, shown as P_1 , P_2 and P_3 .

2.2.1. Design variation analysis of $pg_{6,2}$. Consider a pmg unit cell with lattice translation vectors \mathbf{a} and \mathbf{b} . Having shown [13] that a $pg_{2,2}$ variation of the Miura-ori does not exist, we intend to find a variation of the Miura-ori by applying a minimal enlargement in the x -direction on the $pg_{2,2}$ unit cell. The minimal enlargement in the x -direction which retains the symmetry group of a pg pattern is $\mathbf{a}' = 3\mathbf{a}$. For a Miura fold pattern, this unit cell is called $pg_{6,2}$. State (0) in figure 15 shows a $pg_{6,2}$ unit cell on a Miura fold pattern in its original configuration. There are six distinct orbits of nodes associated with the unit cell. In State (1), we have perturbed the pattern using all degrees of freedom.

According to our studies, in general, $pg_{6,2}$ is not an easily constructible variation of the Miura-ori. In fact, the problem gets increasingly complex as we increase the number of orbits of nodes. Nevertheless, we have developed a computer code which finds solutions for $pg_{6,2}$ through minimizing the total flat-foldability error. Consider a symmetric perturbation of the Miura-ori shown in State (1) of figure 15. Denoting the flat-foldability error (defined [14] as the sum of opposite angles

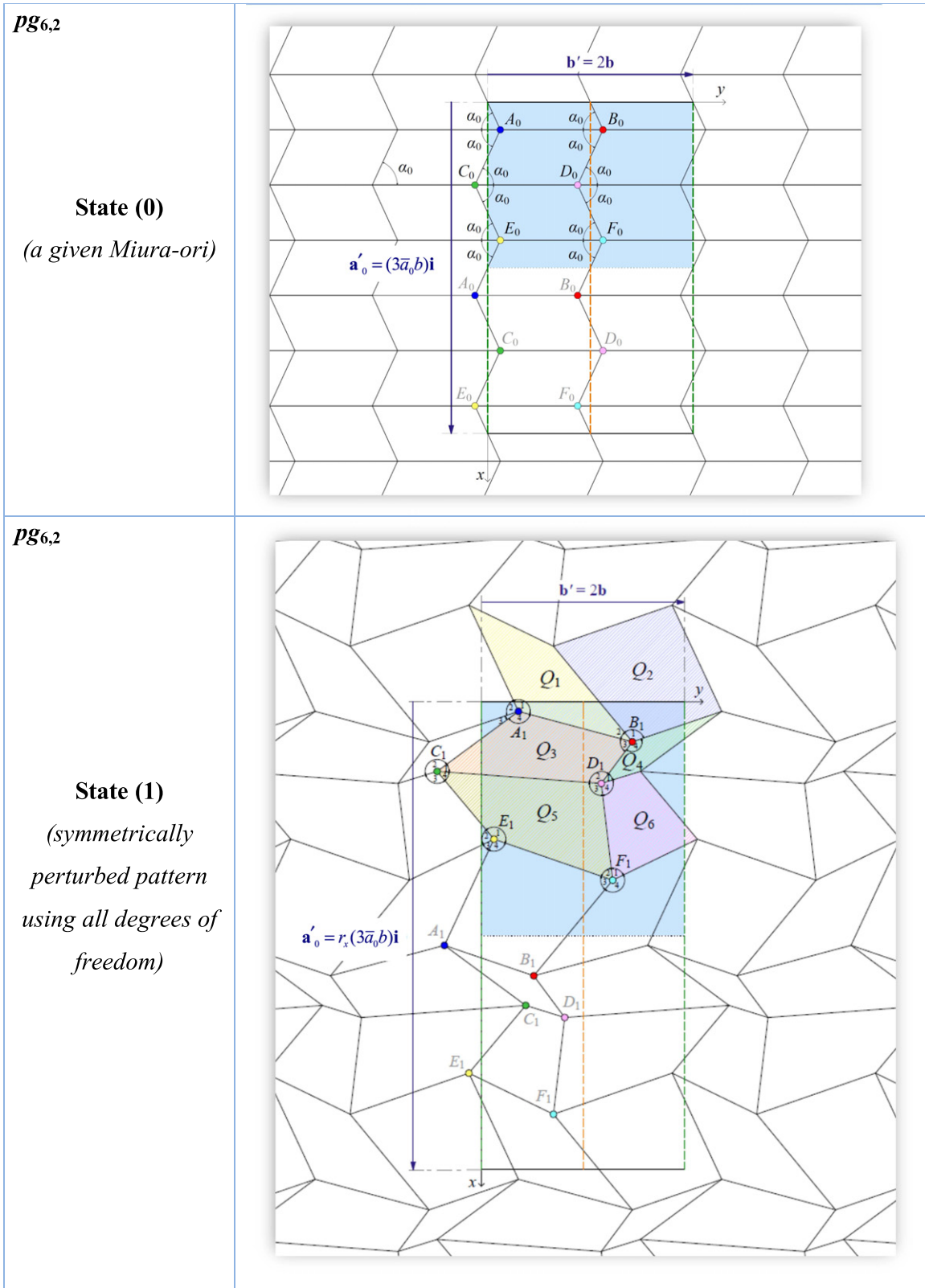


Figure 15. A *pg*_{6,2} variation of the Miura-ori. State (0): a given Miura fold pattern. State (1): a perturbed state using all degrees of freedom. There are six different starting convex quadrilaterals in the pattern, shown as Q_1, Q_2, \dots, Q_6 . State (1) is not flat-foldable in general; we present a flat-foldable variation of it later in this section.

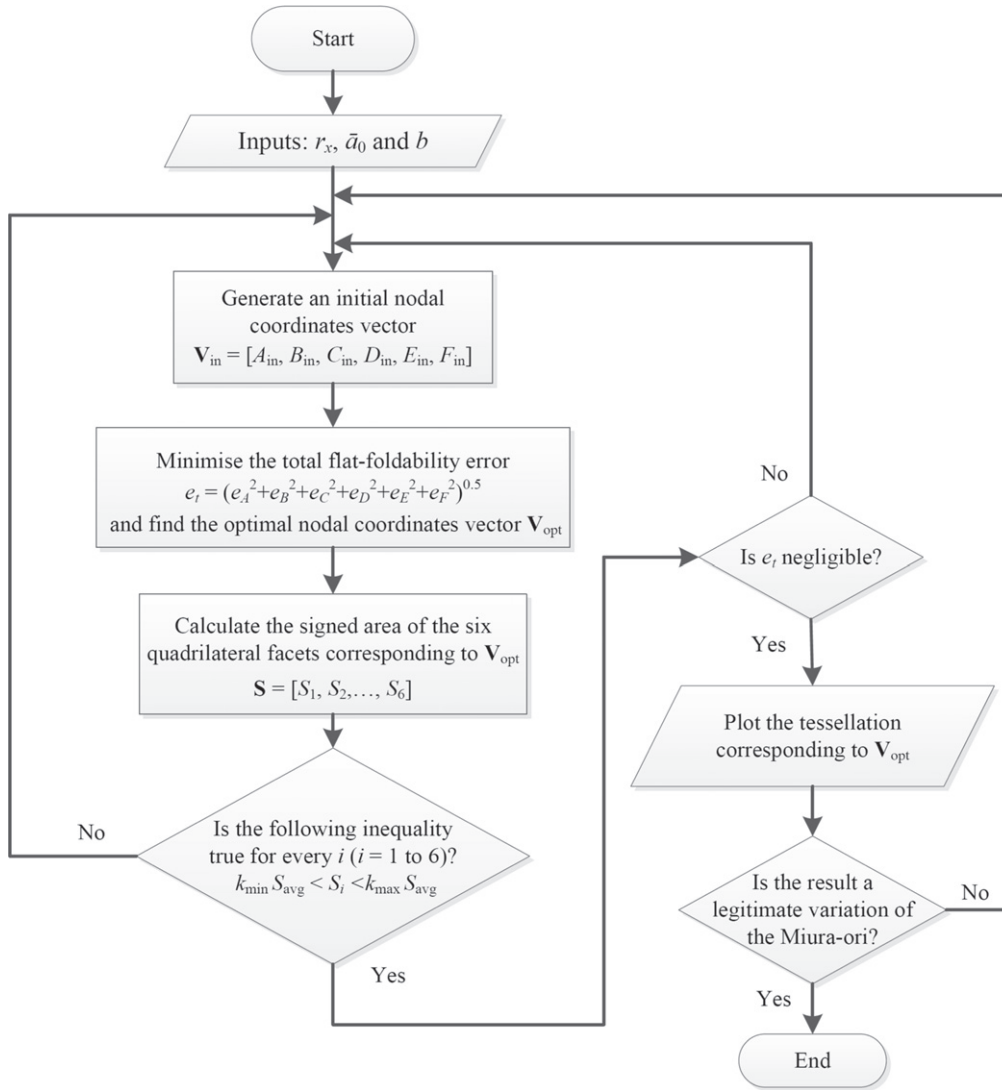


Figure 16. Flowchart of the computational design generation process of the $pg_{6,2}$ variation of the Miura-ori. Outputs are checked to be legitimate [1] variations.

minus π) at nodes A_1, B_1, C_1, D_1, E_1 and F_1 as e_A, e_B, e_C, e_D, e_E and e_F , respectively, the total flat-foldability error e_t of the tessellation is defined as:

$$e_t = \sqrt{e_A^2 + e_B^2 + e_C^2 + e_D^2 + e_E^2 + e_F^2} \quad (21)$$

which is the objective function to be minimized. Assuming that we are given a fixed unit cell (so r_x, \bar{a}_0 and b are fixed), we intend to find a vector \mathbf{V} containing the coordinates of the six nodes associated with the fundamental region of the unit cell:

$$\mathbf{V} = [A, B, C, D, E, F]. \quad (22)$$

In order to avoid undesirable answers from our programme in which some of the quadrilaterals are self-intersecting, we use the concept of *signed* or *algebraic area*. By convention, the signed area of a triangle is positive if it is oriented counter-clockwise, and is negative if it is clockwise. The signed area of a polygon is the sum of the signed areas of the triangles which can be obtained by drawing its diagonals

(see, e.g., [15] for more details). We define a vector \mathbf{S} containing the signed area of the six quadrilateral facets:

$$\mathbf{S}(r_x, \bar{a}_0, b, \mathbf{V}) = [S_1, S_2, \dots, S_6]. \quad (23)$$

The area of a perturbed $pg_{6,2}$ unit cell is (UC stands for unit cell):

$$S_{UC} = a' b' = 6r_x \bar{a}_0 b^2. \quad (24)$$

Knowing that $S_{FR} = \frac{1}{2} S_{UC}$, where FR stands for fundamental region, we have:

$$S_{FR} = 3r_x \bar{a}_0 b^2. \quad (25)$$

Using a unit cell recomposition process (see [1] or [4]), we conclude that the sum of the areas of the six quadrilateral facets is equal to the area of the fundamental region:

$$\sum_{i=1}^6 S_i = S_{FR}. \quad (26)$$

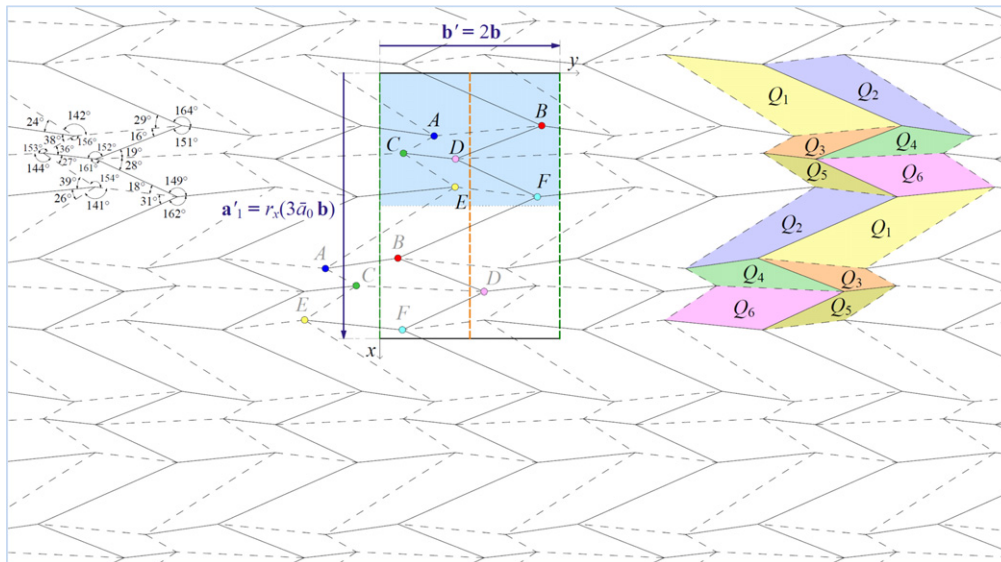


Figure 17. An example for a flat-foldable $pg_{6,2}$ variation of the Miura-ori emerged from the computational design algorithm presented in figure 16. It consists of six different starting convex quadrilaterals, shown as Q_1, Q_2, Q_3, Q_4, Q_5 and Q_6 . Solid lines show mountain fold lines, while dashed lines represent valley fold lines.

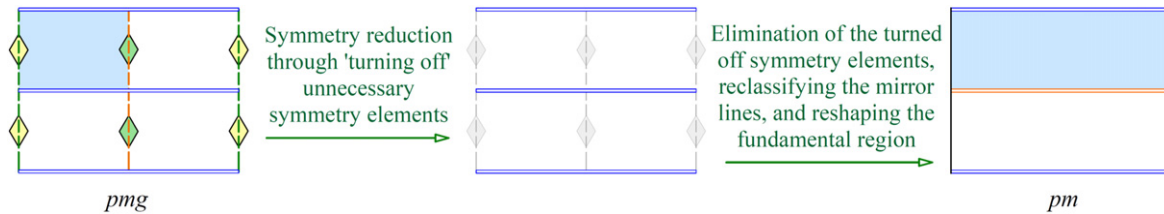


Figure 18. The transformation process of a pmg unit cell into a pm unit cell. The symmetry elements which are turned off are shown in grey.

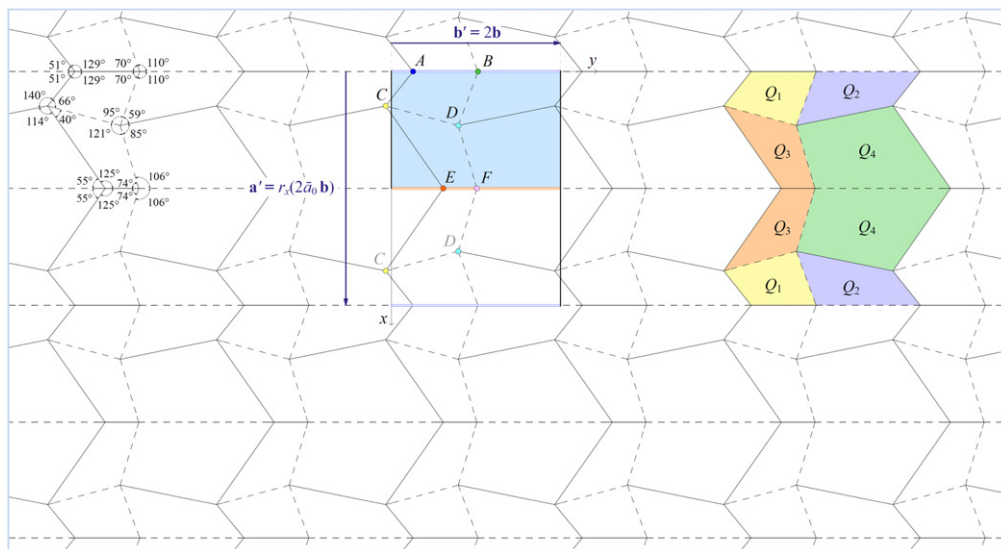


Figure 19. An example for a flat-foldable $pm_{4,2}$ variation of the Miura-ori. It consists of four different starting convex quadrilaterals, shown as Q_1, Q_2, Q_3 and Q_4 . Solid lines show mountain fold lines, while dashed lines represent valley fold lines.

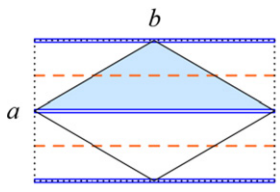
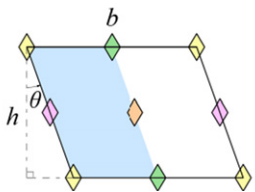
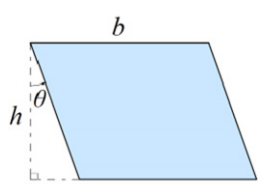
The average area of the quadrilateral facets is:

$$S_{avg} = \frac{1}{6} \sum_{i=1}^6 S_i = \frac{1}{2} r_x \bar{a}_0 b^2. \tag{27}$$

In order for the programme to return useful and reasonable results, we add the following constraint to the minimization process:

$$k_{min} S_{avg} < S_i < k_{max} S_{avg} \quad (1 \leq i \leq 6), \tag{28}$$

Table 1. The subgroups of pmg with non-rectangular unit cells. The bold solid lines depict the borders of the unit cells. The bold dotted lines for the group cm represent the borders of the centred cell of the pattern. The blue shaded areas show the fundamental regions of the unit cells. Double and dashed lines represent reflection and glide reflection axes, respectively. 2-fold axes are shown by rhombuses. The number of degrees of freedom (DOFs) are given to define the shape of the unit cell.

	Rhombic unit cell	Parallelogram unit cells	
Group name	cm	$p2$	$p1$
Unit cell layout			
DOFs	a/b	h/b and θ	h/b and θ
Number of DOFs	1	2	2

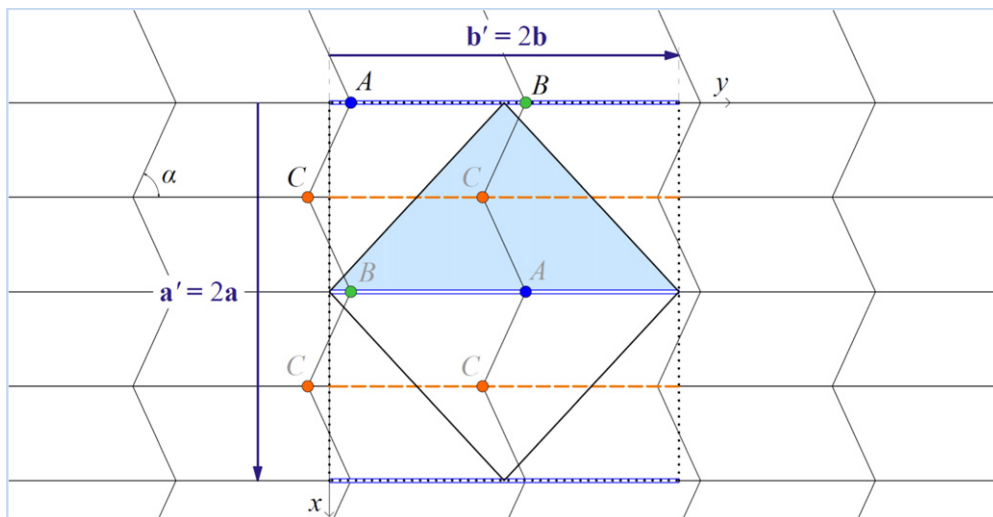


Figure 20. A $cm_{4,2}$ unit cell contains three distinct orbits of nodes, shown as A , B and C .

where k_{min} and k_{max} are the lower and upper multiplication factors, respectively, chosen by the user and applied to the average facet area. The flowchart of the computational design generation process of the $pg_{6,2}$ variation of the Miura-ori is depicted in figure 16.

Our investigations show that we are unlikely to obtain solutions for randomly selected initial points. However, if we use reasonably small random deviations from the nodal coordinates of a flat-foldable $pmg_{6,2}$ variation of the Miura-ori (sharing the same unit cell aspect ratio) as the initial points, the optimization function converges to a solution which is a flat-foldable strictly $pg_{6,2}$ variation of the Miura-ori. Figure 17 shows an example for a computationally generated flat-foldable $pg_{6,2}$ variation of the Miura fold pattern, alongside the assigned mountains and valleys. The pattern consists of six different starting convex quadrilaterals, shown as Q_1, Q_2, \dots, Q_6 .

Adding the global planarity constraint to the problem decreases the number of degrees of freedom and makes the pattern constructible using a ruler and a protractor. An example for a flat-foldable planar $pg_{6,2}$ variation of the Miura fold pattern is presented in [13].

2.3. Group pm

The last subgroup of pmg with rectangular unit cell which we study in this paper is pm . In order to study the symmetry reduction process from pmg to pm , it is easier to use the primary non-standard choice [1] for the pmg unit cell. This unit cell is illustrated again on the left hand side of figure 18, which shows the symmetry reduction transformation of a pmg unit cell into a pm unit cell.

In comparison to the other non-isomorphic variations studied so far, the pm variation of the Miura-ori is easily

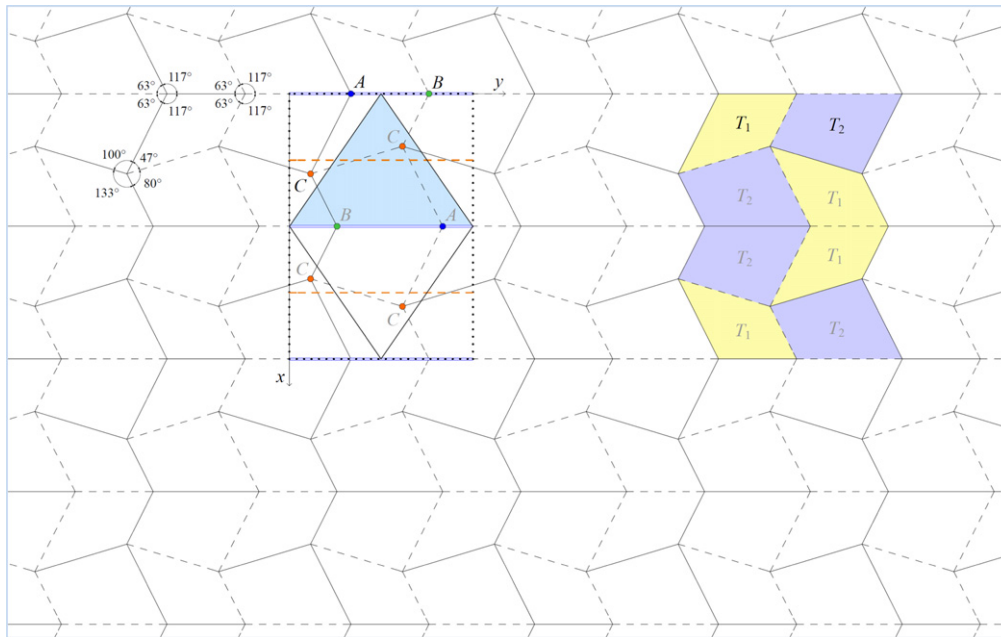


Figure 21. An example for a flat-foldable $cm_{4,2}$ variation of the Miura-ori. It consists of two different starting trapezoids, shown as T_1 and T_2 . Solid lines show mountain fold lines, while dashed lines represent valley fold lines.

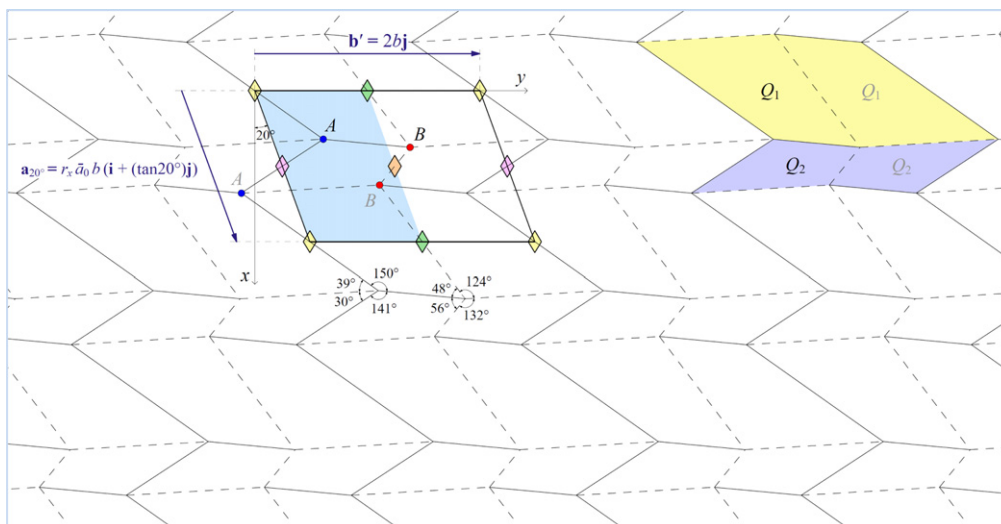


Figure 22. An example for a flat-foldable $(p2)_{2,2}$ variation of the Miura-ori ($\theta = 20^\circ$). It consists of two different starting convex quadrilaterals, shown as Q_1 and Q_2 . Solid lines show mountain fold lines, while dashed lines represent valley fold lines.

generalizable. We have shown [13] that the generalized pm variation of the Miura-ori in both longitudinal and transverse directions simultaneously has the general form $pm_{m,n}$, where $m=2p$, and n and p are natural numbers. It consists of $n(p + 1)$ distinct orbits of nodes and np distinct starting convex quadrilaterals. Figure 19 shows a $pm_{4,2}$ variation of the Miura-ori.

3. Non-isomorphic descendants with non-rectangular unit cells

This section studies the non-isomorphic symmetric variations of the Miura-ori with non-rectangular unit cells, i.e. the plane symmetry groups cm , $p2$, and $p1$. The group cm has a

rhombic unit cell which has one degree of freedom for the unit cell layout, and both groups $p1$ and $p2$ possess a parallelogram unit cell with two degrees of freedoms for the unit cell layout. These unit cells are presented in table 1 along with their respective degrees of freedom. The group cm has a rectangular ‘centred cell’ [7] which is twice as large as the rhombic unit cell. This section explores the cm , $p2$ and $p1$ variations of the Miura-ori, respectively.

3.1. Group cm

Consider a pmg unit cell with lattice translation vectors \mathbf{a} and \mathbf{b} . There is not any direct information about the enlarged maximal cm subgroup for this group in the International

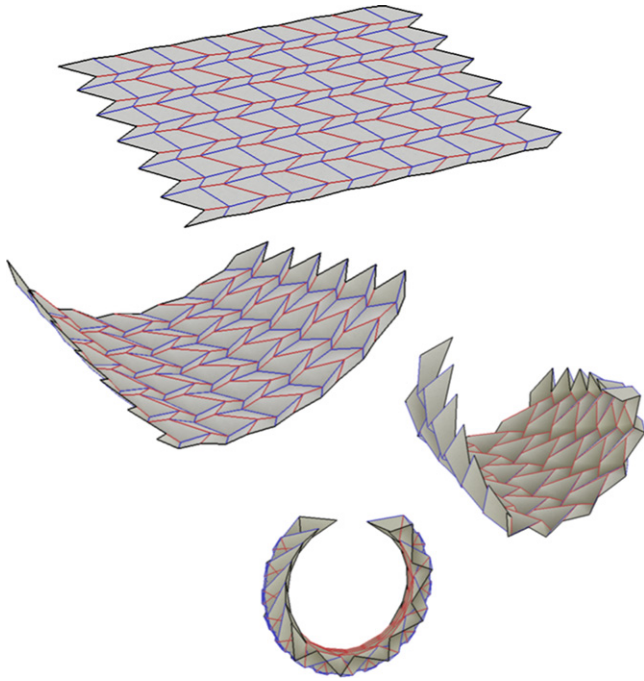


Figure 23. Simulation of the folding process of the $(p2)_{2,2}$ pattern shown in the previous figure, using the Freeform Origami software [16].

Tables for Crystallography [6]. Nevertheless, we can extract this information from the data available for the group pm , according to which the maximal cm subgroup for a pm pattern has a unit cell doubled in both x - and y -directions. As we know that the maximal pm subgroup for the Miura-ori (a pmg pattern) has a unit cell with the same size called $pm_{2,1}$, we can conclude that the maximal cm variation of the Miura-ori is $cm_{4,2}$. An important point regarding the group cm is that for a $cm_{X,Y}$ variation of the Miura-ori the number of quadrilaterals

associated with the unit cell is $(X \times Y)/2$, rather than $X \times Y$, owing to the fact that the area of the rhombic unit cell of a cm pattern is half of the area of its rectangular centred cell.

A $cm_{4,2}$ unit cell is shown in figure 20. There are three distinct orbits of nodes associated with the unit cell, shown as A , B and C in the figure.

Starting from the above unit cell, we have designed [13] the $cm_{4,2}$ variation of the Miura-ori, and have shown that all the $cm_{4,2}$ variations of the Miura-ori are globally planar. Figure 21 shows an example for a flat-foldable $cm_{4,2}$ variation of the Miura fold pattern alongside the assigned mountains and valleys. The pattern consists of two different starting trapezoids T_1 and T_2 .

We have also studied (see [13] for more details) minimal variations on the minimal cm variation of the Miura-ori, i.e. $cm_{4,2}$, in the x - and y -directions, respectively. According to the International Tables for Crystallography [6], the maximal isomorphic subgroup of a cm group has either a unit cell with $\mathbf{a}' = 3\mathbf{a}$, or a unit cell with $\mathbf{b}' = 3\mathbf{b}$. For a Miura fold pattern, these unit cells are called $cm_{12,2}$ and $cm_{4,6}$, respectively. Example patterns are presented in [13].

3.2. Group $p2$

Consider a pmg unit cell with lattice translation vectors \mathbf{a} and \mathbf{b} . According to the International Tables for Crystallography [6], the maximal $p2$ subgroup for this group has a unit cell with the same size. We can deduce from the same reference that the maximal isomorphic subgroup for a $p2$ pattern has a unit cell doubled either in the x - or in the y -direction. In general, for a $p2$ wallpaper pattern with a unit cell height h and a base (width) b , it can be shown that a wallpaper pattern with $h' = mh$ or $b' = nb$ is an isomorphic subgroup of the initial unit cell for any natural numbers m and n .

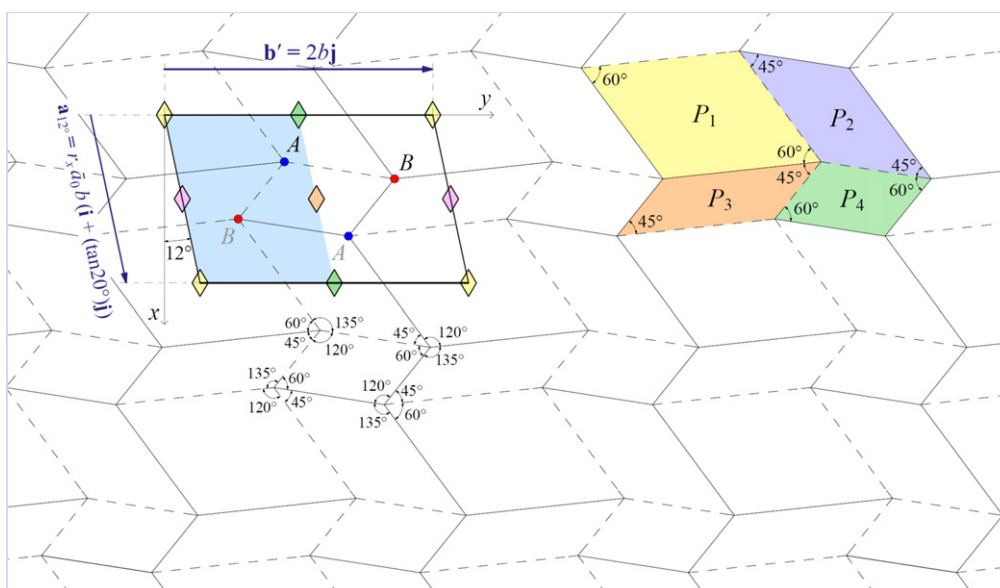


Figure 24. An example for a flat-foldable planar $(p2)_{2,2}^+$ variation of the Miura-ori ($\theta = 12^\circ$). It consists of four different starting parallelograms, shown as P_1 , P_2 , P_3 and P_4 . Solid lines show mountain fold lines, while dashed lines represent valley fold lines.

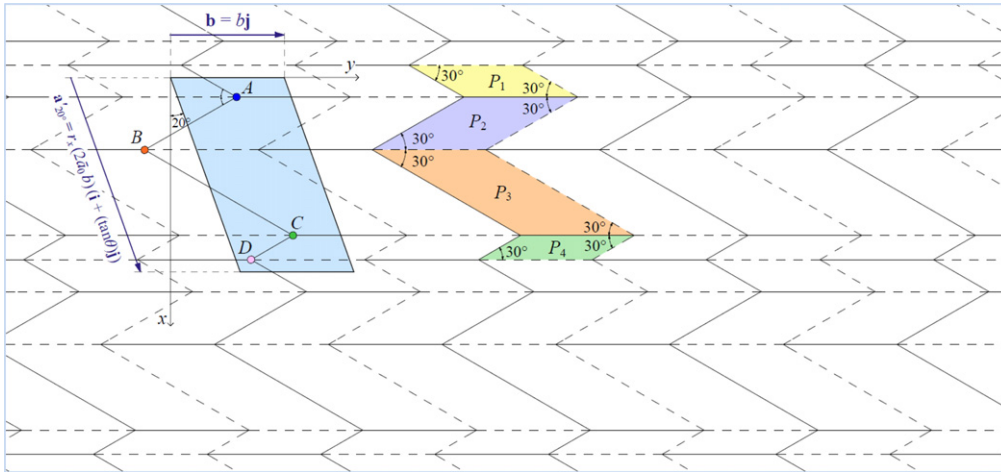


Figure 25. An example for a flat-foldable $(p1)_{4,1}$ variation of the Miura-ori ($\theta = 20^\circ$). It consists of four different starting parallelograms, shown as P_1 , P_2 , P_3 and P_4 . Solid lines show mountain fold lines, while dashed lines represent valley fold lines.

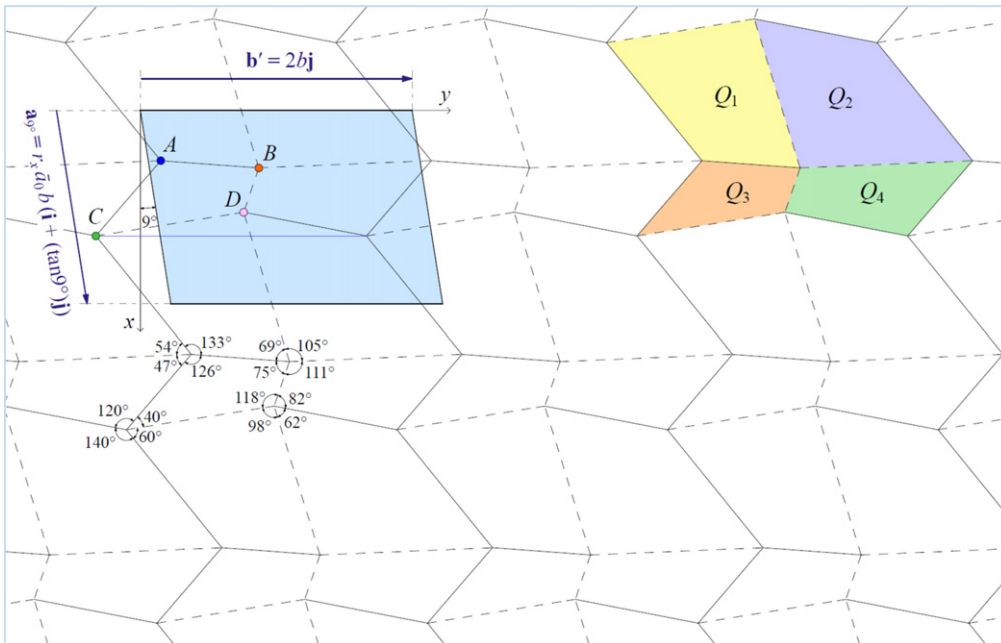


Figure 26. An example for a flat-foldable $(p1)_{2,2}$ variation of the Miura-ori ($\theta = 9^\circ$). It consists of four different starting convex quadrilaterals, shown as Q_1 , Q_2 , Q_3 and Q_4 . Solid lines show mountain fold lines, while dashed lines represent valley fold lines.

Various $p2$ descendants of the Miura-ori are studied in [13]. As an example, a flat-foldable $(p2)_{2,2}$ variation of the Miura-ori is shown in figure 22. A computer simulation of the folding process of this pattern is depicted in figure 23. As can be seen from this figure, the pattern is globally curved. As another example, a flat-foldable $(p2)_{2,2}^+$ variation of the Miura-ori is shown in figure 24. This pattern is an *inclined Miura-ori* [1].

3.3. Group $p1$

The group $p1$ is the least symmetric wallpaper group. The unit cell variation scheme for this group is similar to the group $p2$

discussed in the previous section. Various $p1$ descendants of the Miura-ori are investigated in [13]. It has been shown that a $(p1)_{2,1}$ variation of the Miura-ori does not exist. Figure 25 shows an example for a flat-foldable $(p1)_{4,1}$ variation of the Miura fold pattern alongside the assigned mountains and valleys. The pattern consists of four different starting parallelograms, shown as P_1 , P_2 , P_3 and P_4 .

Figure 26 shows an example for a flat-foldable $(p1)_{2,2}$ variation of the Miura fold pattern, alongside the assigned mountains and valleys. The pattern consists of four different starting convex quadrilaterals, shown as Q_1 , Q_2 , Q_3 and Q_4 .

4. Conclusions

Based on the subgroup relationships among the plane symmetry groups, and using a previously developed framework for symmetric generalization of the Miura-ori, we studied non-isomorphic symmetric variations on this pattern. We started with the Miura-ori and reduced its symmetry by migrating from pmg to its subgroups, which may also include the enlargement of its unit cell. We explored possible flat-foldable non-isomorphic descendants for the Miura-ori, and presented example fold patterns for possible variations.

References

- [1] Sareh P and Guest S D 2015 A framework for the symmetric generalisation of the Miura-ori *Int. J. Space Struct. Spec. Issue Folds Struct.* at press
- [2] Miura K 1994 Map fold a la Miura style, its physical characteristics and application to the space science *Research of Pattern Formation* ed R Takaki (Tokyo: KTK Scientific Publishers) pp 77–90
- [3] Sareh P and Guest S D 2013 Minimal isomorphic symmetric variations on the miura fold pattern *Transformables 2013: Proc. 1st Int. Conf. on Transformable Architecture (Seville, Spain)*
- [4] Sareh P and Guest S D 2015 Design of isomorphic symmetric descendants of the Miura-ori *Smart Mater. Struct.* **24** 085001
- [5] Schwarzenberger R L E 1974 The 17 plane symmetry groups *Math. Gaz.* **58** 123–31
- [6] Hahn T 2005 International tables for crystallography vol A *Space-Group Symmetry* (New York: Springer)
- [7] Schattschneider D 1978 The plane symmetry groups: their recognition and notation *Am. Math. Mon.* **85** 439–50
- [8] Coxeter H S M 1989 *Introduction To Geometry* 2nd edn (Hoboken, NJ: Wiley)
- [9] Martin G E 1996 *Transformation Geometry: An Introduction to Symmetry* 4th edn (New York: Springer)
- [10] Coxeter H S M and Moser W O J 1972 *Generators and Relations for Discrete Groups* 3rd edn (Berlin: Springer)
- [11] Liu Y and Collins R T 2001 Skewed symmetry groups *CVPR 2001: IEEE Computer Society Conf. on Computer Vision and Pattern Recognition (Kauai, HI, USA)*
- [12] Sareh P and Guest S D 2014 Designing symmetric derivatives of the Miura-ori *Advances in Architectural Geometry* (London: Springer) pp 233–41
- [13] Sareh P 2014 Symmetric descendants of the Miura-ori *PhD Dissertation* Engineering Department, University of Cambridge, UK
- [14] Sareh P and Guest S D 2012 Tessellating variations on the Miura fold pattern *IASS: Proc. Int. Association for Shell and Spatial Structures (Seoul, South Korea)*
- [15] Farin G and Hansford D 2013 *Practical Linear Algebra: A Geometry Toolbox* (Boca Raton, FL: A K Peters/CRC Press)
- [16] Tachi T 2013 'Freeform Origami' (online) (www.tsg.ne.jp/TT/software/)